PEPTIDES 29 (2008) 1505–1513

available at www.sciencedirect.com

ScienceDirect

journal homepage: www.elsevier.com/locate/peptides

Expression and characterization of LTx2, a neurotoxin from *Lasiodora* sp. effecting on calcium channels

A.A. Dutra [a], L.O. Sousa [a], R.R. Resende [b], R.L. Brandão [a], E. Kalapothakis [c], I.M. Castro [a,*]

[a] Laboratório de Biologia Celular e Molecular, Núcleo de Pesquisa em Ciências Biológicas, Departamento de Farmácia, Universidade Federal de Ouro Preto, Ouro Preto, MG 35400.000, Brazil

[b] Departamento de Fisiologia e Biofísica, Instituto de Ciências Biomédicas, Universidade de São Paulo, São Paulo, Brazil

[c] Laboratório de Biotecnologia e Marcadores Moleculares, Departamento de Biologia Geral, Instituto de Ciências Biológicas, Universidade Federal de Minas Gerais, Belo Horizonte, MG 31270.901, Brazil

ARTICLE INFO

Article history:
Received 29 February 2008
Received in revised form
29 April 2008
Accepted 1 May 2008
Published on line 7 May 2008

Keywords:
Spider toxins
Lasiodora
cDNA
Expression
Calcium channel
Venom

ABSTRACT

Here, we described the expression and characterization of the recombinant toxin LTx2, which was previously isolated from the venomous cDNA library of a Brazilian spider, *Lasiodora* sp. (Mygalomorphae, Theraphosidae). The recombinant toxin found in the soluble and insoluble fractions was purified by reverse phase high-performance liquid chromatography (HPLC). Ca^{2+} imaging analysis revealed that the recombinant LTx2 acts on calcium channels of BC3H1 cells, blocking L-type calcium channels.

1. Introduction

Previously studied animal toxins have been found to target neuronal receptors, neuronal ion channels and presynaptic membrane proteins involved in transmitter release [30]. Toxins that modulate ion channels represent a key class of pharmaceutical agents [9,12]. Natural toxins that interact with specific receptors may block the excitation of muscles leading to flaccid paralysis and death. These are desired features for pesticides [1,29].

The Brazilian *Lasiodora* spider, commonly known as ''caranguejeiras'', inhabits southeastern Brazil. While the venom is not considered hazardous to humans, the spider's urticating hairs can be allergenic. The crude venom and the two major peptide toxins of *Lasiodora parahybana* (*L. parahybana*) have been shown to be toxic to crickets and mice [11]. Fractions derived from ion exchange high-performance liquid chromatography (HPLC) showed little overlap between vertebrate and invertebrate activity. Although the two toxins (LpTx1 and LpTx2) were isolated and sequenced by Edman degradation, their activity remains unknown. Analysis of *L. parahybana* venom by LC/ESI-QqTof, nanoESI-MS and MALDI-TOF MS provided a peptide profile of *L. parahybana* venom [15].

Many spider venoms contain peptide neurotoxins active on ion channels. On the other hand, the importance of Ca^{2+} as a universal signaling agent in processes such as protein secretion, exocytosis, and muscle contraction has been addressed [5]. Most cells utilize two main sources of Ca^{2+} for generating calcium signals, one is Ca^{2+} entry across the plasma membrane and the other is Ca^{2+} release from internal

* *Corresponding author*. Tel.: +55 31 3559 1722; fax: +55 31 3559 1680.
E-mail address: imcastro@nupeb.ufop.br (I.M. Castro).

0196-9781/$ – see front matter
doi:10.1016/j.peptides.2008.05.001

stores. Ca^{2+} release from internal stores occurs primarily from the endoplasmic reticulum (ER) wherein two functionally distinct Ca^{2+} release channels have been identified, namely inositol 1,4,5-trisphosphate receptors ($InsP_3Rs$) and ryanodine receptors (RyRs) [3,4]. Ca^{2+} entry across the plasma membrane occurs via two distinct pathways, voltage-gated Ca^{2+} channels (VGCCs), and agonist-dependent and voltage-independent Ca^{2+} entry pathways, which are called 'store-operated' Ca^{2+} (SOCs) channels [5].

In the current study, venom was obtained from *Lasiodora* sp. collected around Belo Horizonte in the state of Minas Gerais, Brazil. *Lasiodora* sp. venom has been shown to contain pharmacological components that inhibit L-type Ca^{2+} channels and modulate Na^+ channels [18,21]; however, these previous studies analyzed crude venom. Molecular cloning of cDNAs that code for the putative toxins produced by this spider can make direct recombinant protein studies possible. The aim of the present work was to express and characterize the LTx2 toxin from *Lasiodora* sp. to further our understanding on the mechanism of action of this spider's venom. To this end, cDNA encoding the LTx2 was inserted into the expression vector pET11a and the translated protein was expressed and purified for functional characterization. Initially, the types and functions of Ca^{2+} channels in plasma membrane and internal Ca^{2+} stores in BC3H1 cells were examined, by Ca^{2+} imaging experiments, as well as the possible involvement of $InsP_3Rs$ or RyRs, and VGCCs or SOCs channels, in $[Ca^{2+}]_i$ oscillations. Additionally, we provide evidence that LTx2 toxin blocks L-type Ca^{2+} channels and inhibits the refill of intracellular Ca^{2+} store, eliminating the $InsP_3$ promoting $[Ca^{2+}]_i$ oscillations.

2. Materials and methods

2.1. Reagents

All reagents were purchased from Sigma (St. Louis, MO) in highest available purity, if not otherwise indicated. Primers used for RT-PCR reactions were purchased from Integrated DNA Technologies (Coralville, IA).

2.2. General molecular biology

Standard recombinant DNA techniques (e.g., phenol extraction, ethanol precipitation and electrophoresis) were carried out as described by Sambrook et al. [35].

2.2.1. DNA sequencing and computer analysis

Small-scale plasmid isolation from *E. coli* was carried out using the alkaline lysis SDS method [35] and purified using Millipore Multiscreen plates (Millipore). DNA sequencing reactions were performed on both strands using chain termination [36]. All reactions were carried out using the MegaBace 500 Sequencing Analysis System and DyEnamic™ ET dye terminator kit. Nucleic acids sequences were compared to sequences in the GenBank database [2].

2.2.2. Expression of toxin in E. coli

The plasmid pET11a (Novagen®) was used to express the mature LTx2 toxin (GenBank accession no. AY794220). The insert was prepared using a polymerase chain reaction (PCR) with forward (5′-C**CATATG**CTTTTCGAATGTAC-3′) and reverse (5′-G**GGATCC**CTAAATCTTCAAAC-3′) primers. The forward PCR primer contained an Nde I restriction site including the translation initiation ATG codon, and the reverse primer had a BamH I site at the 3′ end immediately after the stop codon. PCR conditions included 34 cycles with each cycle with 94 °C for 1 min, followed by 52 °C for 1 min, and 72 °C for 1 min. The reaction was concluded with a 5 min elongation phase at 72 °C. The gel-purified PCR product was digested with Nde I/BamH I and ligated into the Nde I/BamH I digested pET11a vector to produce the expression plasmid pET11a-LTx2.

Competent *E. coli* strain BL21 (DE3) cells were transformed with the recombinant plasmid. The presence of the appropriate insert was determined using direct colony PCR and DNA sequencing. Bacterial growth, induction with isopropyl β-D-1-thiogalactopyranoside (IPTG) and preparation of cell lysates were performed as described by the manufacturer (Novagen®). Briefly, stocked cultures of transformants were grown in 4.0 ml of LB-ampicillin medium. One milliliter of inoculum was added to 100 ml fresh medium and incubated until the OD 600 was 0.5–0.7. Protein expression was induced by addition of 0.6 mM IPTG and the cultures were grown for 6 h at 30 °C. Cells were harvested by centrifugation and resuspended in 10 ml lysis buffer (50 mM Tris pH 8.0, 100 mM NaCl, 10 mM imidazole, lysozime 1 mg ml^{-1} plus proteases inhibitors (1 mM PMSF, 1 mM iodacetamide, 1 μg ml^{-1} pepstatin, 1 mM EDTA)). The cells were lysed by sonication on ice. After centrifugation at 20,000 × *g*, both fractions – soluble and inclusion bodies – were stored for further tests. Protein content was estimated by the Bradford's protein assay [6] and samples were analyzed by SDS-PAGE.

2.2.3. SDS-PAGE and immunoblot

Proteins samples were prepared and separated by electrophoresis on 18% acrylamide gels [22]. Gels were run at 100 V for 1 h and stained with Coomassie Blue G-250 or transferred to a nitrocellulose membrane for immunolabeling [14] using anti-*Lasiodora*-venom antibodies.

2.3. Purification of recombinant LTx2

The LTx2 recombinant protein was purified from inclusion bodies. Protein refolding was carried out as described by Roberto et al. [33]. Reverse-phase chromatography was performed using a PEPMap C8 prepacked column and an HPLC Acta™ Explorer System (Amersham Biosciences, Uppsala, Sweden). After equilibrating the column with 0.1% trifluoroacetic acid (TFA)/deionized water (mobile phase), the protein was eluted with a continuous gradient of a mobile phase containing acetonitrile/0.1% TFA. The eluant profile was monitored continuously at 280 and 214 nm. The fractions were then dialyzed, lyophilized and stored at −20 °C.

2.4. Pharmacological characterization

2.4.1. Calcium oscillations in BC3H1 cells

2.4.1.1. Cell culture. BC3H1 cells expressing muscle-type acetylcholine receptors (AChRs) [38] were cultured as described elsewhere [39]. Briefly, cells were maintained in

Dulbecco's modified Eagle's medium (DMEM, Invitrogen, Carlsbad, CA) supplemented with 10% fetal bovine serum (FBS, Cultilab, Campinas, Brazil), 100 units ml^{-1} penicillin, 100 (g ml^{-1} streptomycin, and 2 mM L-glutamine. For experiments, 2.3×10^5 BC3H1 cells ml^{-1} were resuspended into 20 ml of 10% FBS medium. The suspension was mixed and 2 ml aliquots were pipetted into each dish. The medium was changed to 1% FBS 24 h after plating on bacterial dishes.

2.4.2. *Calcium measurements*

BC3H1 cells were loaded with Fluo-3-AM by incubation with 4 μM Fluo-3-AM in 0.5% Me_2SO and 0.1% of the non-ionic surfactant pluronic acid F-127 for 30 min at 37 °C in 140 mM NaCl, 3 mM KCl, 1 mM $MgCl_2$, 2.5 mM $CaCl_2$, 10 mM HEPES, and 10 mM glucose at pH 7.4. After loading with Fluo-3-AM, the cells were washed with incubation buffer and incubated for 20 min to ensure complete de-esterification of the dye. Ca^{2+} imaging was performed with an LSM 510 confocal microscope (Zeiss, Jena, Germany). Fluo-3 fluorescence emission was excited with a 488 nm line from an argon ion laser and the emitted light at 515 nm was detected using a band pass filter. At the end of each experiment, 5 μM of the ionophore (4-Br-A23187) followed by 10 mM EGTA were used to determine maximal (F_{max}) and minimal (F_{min}) fluorescence values. Ca^{2+} concentration was calculated from the Fluo-3 fluorescence emission using a self-ratio equation as described previously [16,31,32] assuming a K_d of 450 nM [17]. The Ca^{2+} imaging data were obtained at 20–22 °C. The osmolarity of all the solutions ranged between 298 and 303 mosmol l^{-1}. Concentrations were calculated for cell populations containing at least 10 cells in three different experiments.

To evaluate the contribution of VGCC activation to the studied Ca^{2+} signals, the depolarizing stimuli were delivered in the presence of the non-selective VGCC and SOC blocker (100 μM Cd^{2+}). Before testing the effects of Cd^{2+}, we evaluated the stability of Ca^{2+} responses to depolarizing stimuli repeated at 5-min intervals. The amplitude of the $\Delta F/F$ ratios in response to the first four stimulations remained fairly stable; those of the third and fourth transients were, respectively, $4.6 \pm 1.8\%$ ($n = 42$) and $7.3 \pm 1.9\%$ ($n = 39$) smaller than that of the first.

Table 1 – Primers for amplification of IP_3Rs, RyRs receptors subtypes and α-subunits of VGCCs by PCR

Gene	Access number	Primer	Sequence (5′-3′)	Length (bp)
IP3R1	NM_010585	FWD	5′CCA TCA ATG AAA TAT CCG GGC A3′	269
		REV	5′AAC TCC ATC GTC TGA GCA3′	
IP3R2	NM_019923	FWD	5′GTT ACA GGA TGT CGT GGC CT3′	333
	NM_0105868	REV	5′AGA GGT CCG TTC ACA CTA AT3′	
IP3R3	NM_080553	FWD	5′TCA CGA GTA CCT CAG CAT CG3′	360
		REV	5′AAC TTG ACA GGG GTC ACC AG3′	
RYR1	NM_009109	FWD	5′TCA CGA GTA CCT CAG CAT CG3′	234
		REV	5′AAC TTG ACA GGG GTC ACC AG3′	
RYR2	NM_023868	FWD	5′ACA ACC CAA ATG CCG GCC TC3′	414
		REV	5′TAG GCA GCT CCT TTC CTT CA3′	
RYR3	NM_177652	FWD	5′TAG CCC AGT AGA AGA GGC CA3′	377
		REV	5′CAC ACT TCA TAT CCG GCT CA3′	
α-Subunit L-type				
1.2	CACNA1C	FWD	5′TCGTGGGTTTCGTCATTGTCA 3′	481
		REV	5′CCTCTGCACTCATAGAGGGAGAG 3′	
1.3	CACNA1D	FWD	5′GAGCCTCGATTAGTATAGTGGAATG 3′	217
		REV	5′AGGATGCAGCAACAGTCCATA 3′	
1.4	CACNA1F	FWD	5′GAAGCAGCAGATGGAAGAAG 3′	206
		REV	5′TGTGTGGAGCGAGTAGAGTG 3′	
P/Q, N, R types				
2.1	CACNA1A	FWD	5′GAGCGGCTGGATGACACGGAACC 3′	420
		REV	5′GAGCTGGCGACTCACCCTGGATGTC 3′	
2.2	CACNA1B	FWD	5′GAAGTAGCTGAAGTCAGCC 3′	483
		REV	5′CTTGCGTGTCAGCCCCTGGA 3′	
2.3	CACNA1E	FWD	5′GAGACTGTGGTGACTTTTGAGGACC 3′	697
		REV	5′ATAGAGCTATGGGGCACCATGGCTT 3′	
T-type				
3.1	CACNA1G	FWD	5′TACGGAGGCTGGAGAAAA 3′	449
		REV	5′GATGATGGTGGG(A/G)TTGAT 3′	
3.2	CACNA1H	FWD	5′CGCAGACTATTCACACAC 3′	325
		REV	5′GATGATGGTGGG(A/G)TTGAT 3′	
3.3	CACNA1I	FWD	5′GGAAAAGAAGCGCCGTAA 3′	364
		REV	5′GATGATGGTGGG(A/G)TTGAT 3′	
β-Actin	NM_007393	FWD	5′AGG AAG AGG ATG CGG CAG TGG 3′	535
		REV	5′ CGA GGC CCA GAG CAA GAG AG 3′	

FWD = forward primer; REV = reverse primer.

2.4.3. Reverse transcription and conventional PCR

Total RNA was isolated using TRIzol (Invitrogen) from undifferentiated BC3H1 cells. Integrity of the isolated RNA was verified by separation on a 2% ethidium bromide-stained agarose gel. DNA was removed from RNA samples by incubation with DNase I (Ambion Inc., Austin, TX).

Primer sequences for reverse transcription and PCR amplification of β-actin, $InsP_3Rs$ and RyRs isoforms mRNA are listed in Table 1. Negative controls were realized with water and total RNA non-reverse transcribed. The amplification reaction mixture (50 μl) contained 200 ng of the cDNA sample, 1.25 U of Ampli-Taq DNA polymerase, 1× PCR reaction buffer, 200 mM of each primer, 200 μM dATP, dCTP, dGTP, and dTTP, and 1.5 mM $MgCl_2$ (Applied Biosystems). The thermal cycling conditions included 5 min at 95 °C. Thermal cycling proceeded with 35 cycles of 94 °C for 30 s, 55 °C for 30 s, and 72 °C for 30 s. After amplification, electrophoresis of 10 μl reaction mixture on a 2% NuSive:agarose gel (3:1) (FMC product, Rockland, ME) was visualized under UV illumination after staining with ethidium bromide.

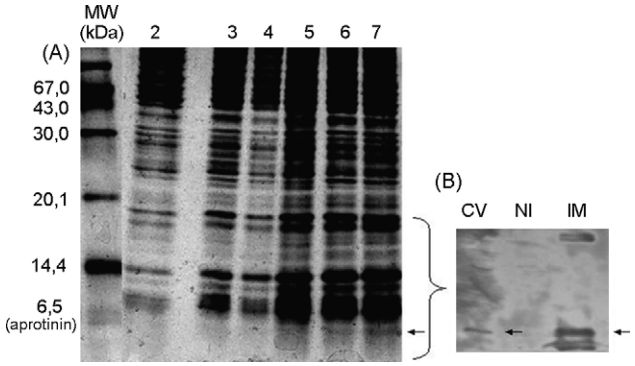

Fig. 1 – (A) SDS-PAGE (18%) profile expression into pET11a(+) induced by IPTG. Each lane was loaded with 20 μg of total protein. (1) Low molecular weight + aprotinin; (2) empty vector; (3) not induced; lanes (4–7) induced for 1, 2, 3 and 4 h with 0.6 mM IPTG, respectively. The arrow shows increases in expression. (B) Immunochemical identification of recombinant LTx2 in bacterial extracts. C.V., crude venom; N.I., not induced; I.M., induced material.

3. Results

3.1. Cloning and expression

The cDNA encoding the mature LTx2 protein was cloned into a pET11a expression vector (pET11a–LTx2), sequenced to confirm the correct frame, and the recombinant toxin was obtained using BL21 (DE3) *E. coli* cells. Fig. 1A shows *E. coli* extracts electrophoresed on an 18% SDS-PAGE after induction with IPTG. A faint band of approximately 5.7 kDa was detected after 4 h of induction, which is consistent with previous studies that deduced molecular weight for this toxin to be ~5.7 kDa. Additionally, immunochemical identification of the recombinant protein using antisera against whole venom is shown in Fig. 1B. A second band just below of 5.7 kDa was detected by Western blot and may correspond to a protein degradation product. Crude venom used as a positive control showed a band with a similar molecular weight. In the negative control (non-induced cells), this band was not observed (Fig. 1B).

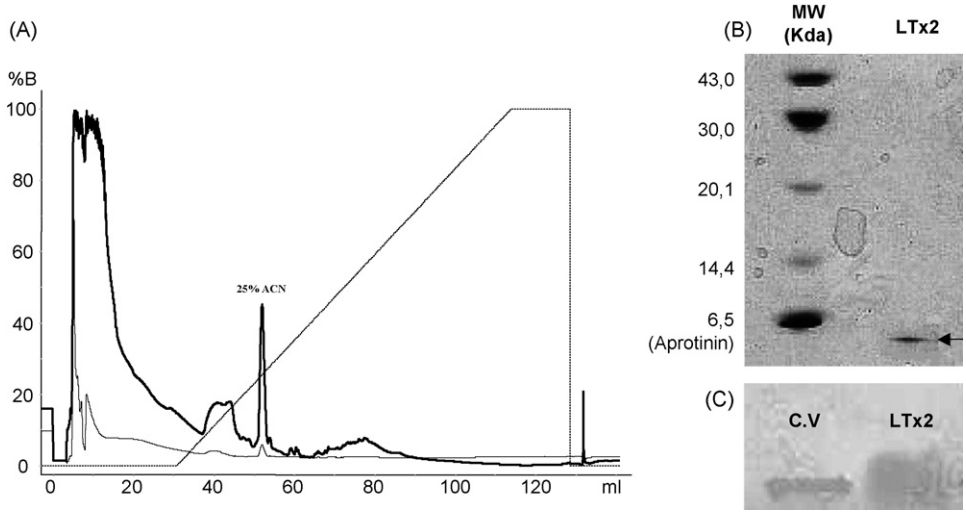

Fig. 2 – (A) HPLC purification of the recombinant LTx2 in a reversed-phase C8 column (Sephasil Peptide C8 5 μ 4.6/205). The thin line represents absorption at 280 nm and the thick line represents absorption at 214 nm. The dotted line corresponds to the acetonitrile gradient (0–100%). Material eluted in the first peaks is the salt present in the sample. The fraction eluted at 25% acetonitrile was analyzed by SDS-PAGE and activity. (B) SDS-PAGE (18%) of the fraction eluted in RP-HPLC. Lane 1: low molecular weight standard added of aprotinine. Lane 2: fraction recovered in RP-HPLC–recombinant LTx2. A single band of approximately 6 kDa is present. (C) Immunochemical identification of the recombinant protein. C.V., crude venom; LTx2, recombinant LTX2.

3.2. *Purification of LTx2 recombinant*

Recombinant LTx2 protein was expressed in transformed *E. coli* (BL21 DE3) and found in both the soluble and insoluble fractions. The LTx2 recombinant protein from the insoluble fraction was solubilized (6 M guanidine hydrochloride, 5% β-mercaptoethanol) and after refolding, was purified in a PepMap C8 RP column (Fig. 2A). The homogeneity of the eluted fraction was demonstrated by SDS-PAGE and Western blot (Fig. 2B and C). The purified protein was demonstrated to be biologically active by calcium imaging in BC3H1 cells (see Sections 3.3.2 and 3.3.3).

3.3. *Activity*

3.3.1. *Ca^{2+} oscillations in BC3H1 cells*

To investigate the dynamics of $[Ca^{2+}]_i$ in BC3H1 cells, we performed Fluo-3 imaging experiments. Spontaneous $[Ca^{2+}]_i$ oscillations were observed in 47 of 62 cells (76%), in external buffer containing 2.5 mM Ca^{2+} without any stimuli (Fig. 3A). Two major pathways control the $[Ca^{2+}]_i$: the Ca^{2+} entry across the plasma membrane and the Ca^{2+} release from internal stores. The contributions of each source of Ca^{2+} to spontaneous $[Ca^{2+}]_i$ oscillations in BC3H1 cells were evaluated. In Ca^{2+}-free buffer, the spontaneous $[Ca^{2+}]_i$ oscillations continued for a while (Fig. 3B). The registered frequencies for $[Ca^{2+}]_i$ oscillation were not statistically different in Ca^{2+}-free buffer and Ca^{2+}-containing buffer (the period was 2.7 ± 1.3 min, $n = 31$, and 4.2 ± 1.2 min, $n = 38$, respectively). Otherwise, the amplitudes of spontaneous $[Ca^{2+}]_i$ oscillation were significantly decreased by $35.7 \pm 3.8\%$ in free-Ca^{2+} buffer ($n = 5$; P-value is <0.05 by paired a t-test). These results indicate that the amplitude, but not the frequency of $[Ca^{2+}]_i$ oscillation, is regulated by Ca^{2+} entry through the plasma membrane. Therefore, we speculated that $[Ca^{2+}]_i$ oscillation may be regulated mainly by Ca^{2+} release from intracellular stores. In order to test this hypothesis, the ER contribution to generate $[Ca^{2+}]_i$ oscillations was examined. First, the effects of the specific Ca^{2+} pump blockers, cyclopiazonic acid (CPA) and thapsigargin (Thaps) were tested. Application of 1 μM Thaps (not shown) or 10 μM CPA inhibited completely $[Ca^{2+}]_i$ oscillations (Fig. 3C), suggesting the involvement of Ca^{2+} release from ER. Two types of Ca^{2+} release channel are present in ER or sarcoplasmic reticulum (SR), RyRs and $InsP_3Rs$. For the next context, the functionality of these receptors in BC3H1 cells was studied. Acetylcholine 100 μM (ACh), in Ca^{2+}-free buffer, which would activate only muscarinic receptors producing $InsP_3$ to activate $InsP_3Rs$, did not induce $[Ca^{2+}]_i$ transients (53 of 58 cells; Fig. 4A), but in external buffer containing Ca^{2+} ACh induced an increase in $[Ca^{2+}]_i$ transients of 778 ± 72 nM ($n = 72$ cells), calculated as reported in Section 2.4.2. We have also tested the effects of the cell-permeant $InsP_3R$ blocker, 2-aminoethoxydiphenyl borate (2-APB), in BC3H1 cells [41]. 2-APB (75 μM) blocked completely spontaneous $[Ca^{2+}]_i$ oscillations (23/23 cells) and, as it was expected, a subsequent application of ACh (100 μM) did not induce any

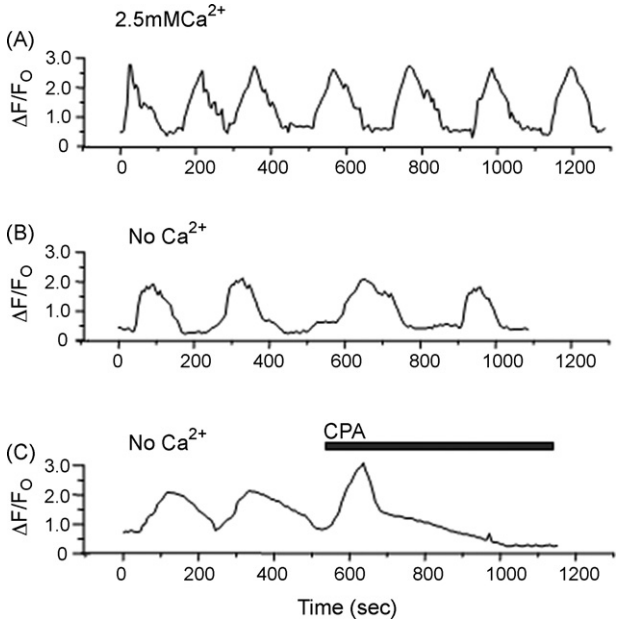

Fig. 3 – Ca^{2+} transients in BC3H1 cells. Cells were loaded with Fluo-3-AM for 30 min. (A) Spontaneous Ca^{2+} oscillations were registered in external buffer containing 2.5 mM Ca^{2+} and (B) in Ca^{2+}-free external buffer (1 mM EGTA). (C) Application of 10 μM cyclopiazonic acid (CPA) blocked completely spontaneous $[Ca^{2+}]_i$ oscillations.

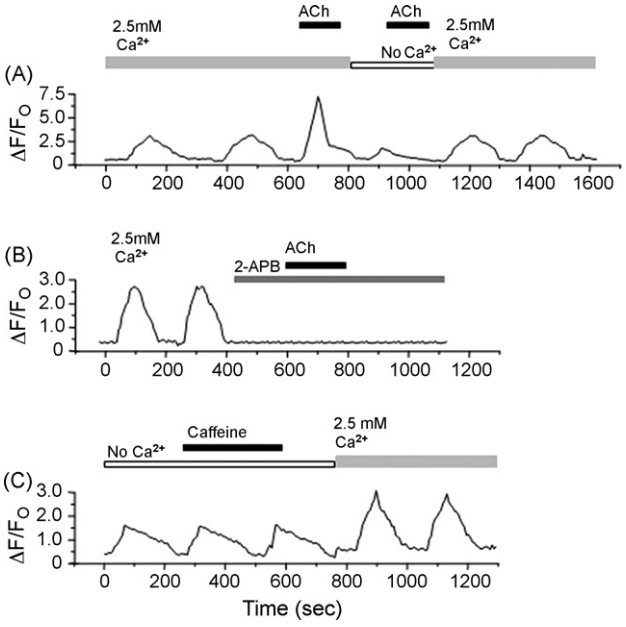

Fig. 4 – Agonist-induced Ca^{2+} release in BC3H1 cells. (A) Addition of 100 μM acetylcholine (Ach)-induced $[Ca^{2+}]_i$ transients in external buffer containing 2.5 mM Ca^{2+}. When we substitute the Ca^{2+}-containing to Ca^{2+}-free buffer and 100 μM ACh was applied, no $[Ca^{2+}]_i$ transient was induced and $[Ca^{2+}]_i$ oscillations was eliminated. When we changed the Ca^{2+}-free to Ca^{2+}-containing buffer $[Ca^{2+}]_i$ increased gradually. (B) After addition of the cell-permeant $InsP_3R$ blocker, 2-APB (75 μM) $[Ca^{2+}]_i$ oscillations were completely blocked and additional application of ACh (100 μM) did not induce any increase of $[Ca^{2+}]_i$. (C) In Ca^{2+}-free buffer, small oscillations were observed. After the application of 10 mM caffeine, Ca^{2+} release from ER could not be induced.

increase of $[Ca^{2+}]_i$ (32/32 cells; Fig. 4B). In contrast, 10 mM caffeine, which activates most forms of RyRs [25] did not affect the level of $[Ca^{2+}]_i$ (54/54 cells, Fig. 4C). The above results suggest that $InsP_3Rs$ mediate the release of Ca^{2+} from ER and generate $[Ca^{2+}]_i$ oscillation in BC3H1 cells.

3.3.2. *Ca^{2+} entry pathways through plasma membrane in BC3H1 cells*

It has been proposed that the main Ca^{2+} entry pathways in non-excitable cells is by SOCs channels, which are activated by Ca^{2+} store depletion [10,28]. However, it is not well understood whether SOCs are present or not in BC3H1 cells, and whether VGCCs channels function in the plasma membrane. Application of 1 μM Thaps in Ca^{2+}-free external buffer induced an increase followed by a decrease in $[Ca^{2+}]_i$ in BC3H. Addition of 2.5 mM Ca^{2+} to the external buffer, evoke a slow increase of $[Ca^{2+}]_i$ (28/28 cells), which indicates Ca^{2+} entry through the plasma membrane (Fig. 5A). In cells treated with 10 μM CPA, the level of $[Ca^{2+}]_i$ increased gradually in the presence of 2.5 mM Ca^{2+} and decreased when the buffer was changed to Ca^{2+}-free buffer. New addition of 2.5 mM Ca^{2+}, resulted in an increase of $[Ca^{2+}]_i$ (32/32 cells; Fig. 5B). These increases of $[Ca^{2+}]_i$ were abolished by the application of an inhibitor for SOC and VGCCs, 100 μM Cd^{2+} (32/32 cells, Fig. 5B), by an inhibitor for L-type Ca^{2+} channel, 5 μM nifedipine (35/35 cells, Fig. 5C), and by 80 μM LTx2 toxin (31/31 cells, Fig. 5D), which suggest that LTx2 toxin act upon these channels. The above results suggest that entry of Ca^{2+} through the plasma membrane is mediated mainly via VGCCs and that LTx2 toxin probably acts upon L-type channels.

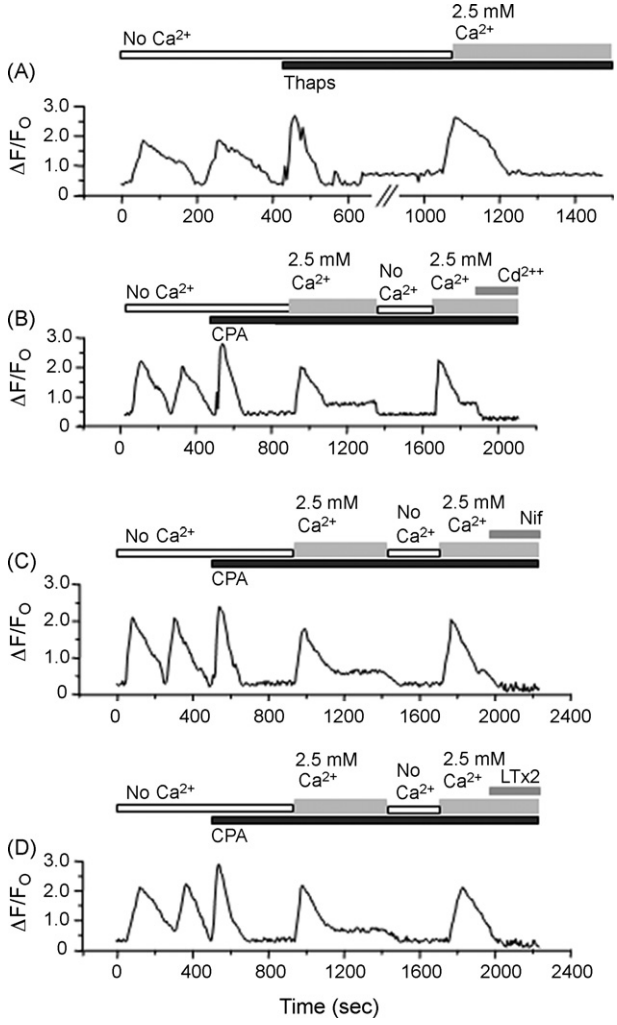

Fig. 5 – Voltage-gated Ca^{2+} channels were activated by depletion of Ca^{2+} store in BC3H1 cells. (A) Application of 1 μM thapsigargin (Thaps) induced a large $[Ca^{2+}]_i$ transient in cells present in Ca^{2+}-free external buffer (no Ca^{2+}). When the Ca^{2+}-free external buffer was changed to 2.5 mM Ca^{2+}-containing buffer $[Ca^{2+}]_i$ increased gradually. (B) When the Ca^{2+} store was depleted with 10 μM cyclopiazonic acid (CPA) $[Ca^{2+}]_i$ decreased markedly. After addition of 2.5 mM Ca^{2+} the $[Ca^{2+}]_i$ increased gradually. Application of 100 μM $CdCl_2$ reduced $[Ca^{2+}]_i$ significantly. (C) The same experiment was done in presence of 5 μM nifedipine (Nif) or (D) 80 μM LTx2. Both, Nif and LTx2 reduced significantly $[Ca^{2+}]_i$.

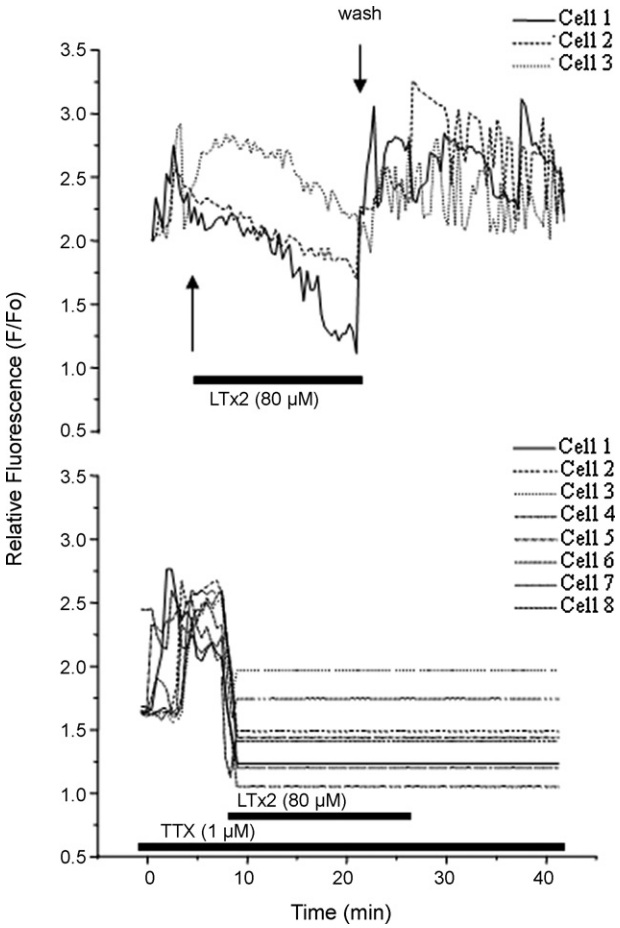

Fig. 6 – $[Ca^{2+}]_i$ oscillations in individual BC3H1 cells observed in the presence of 80 μM recombinant LTx2 with (lower panel) and without (upper panel) 1 μM TTX. BC3H1 cells had Ca^{2+} oscillations before LTx2 was added to bathing medium, even in the presence of TTX. Spontaneous $[Ca^{2+}]_i$ oscillations were abolished and there was a decrease in the basal level of $[Ca^{2+}]_i$ in the presence of 80 μM LTx2 and 1 μM TTX.

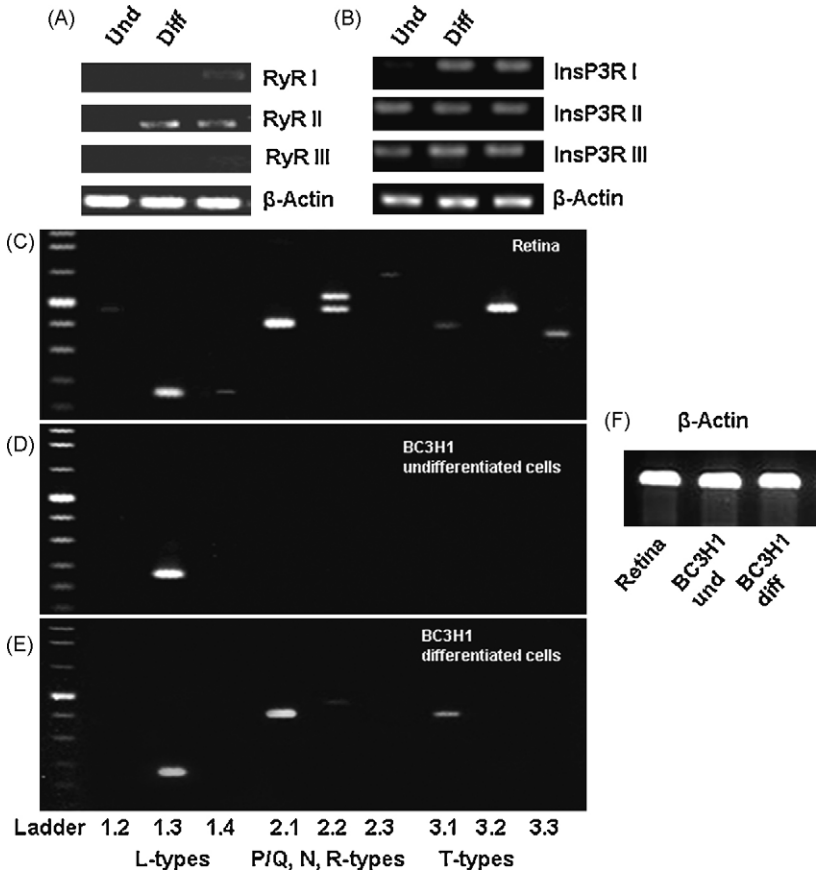

Fig. 7 – mRNA expression: (A) RyR type I, II, and III were evaluated at undifferentiated (Und) and muscle-differentiated (Diff) BC3H1 cells, by RT-PCR. RyR gene was not found in Und stage. (B) InsP$_3$R I, II, and III genes were expressed at detectable levels in both, Und and Diff stage. (C) Expression of VGCC α-subunit encoding mRNAs in control retina cells. Specific subunits of all major classes of VGCCs were found in control cells. (D) α-Subunit mRNAs detected from undifferentiated BC3H1 cell line. A single PCR product (CaV1.3α1; CACNA1D) was observed. (E) Profile of VGCC α-subunit mRNAs present in a muscle-differentiated BC3H1 cells. Genomic amplification was observed for CaV1.3α1, CaV2.1α1 (larger band) and CaV3.1α1. (F) β-Actin control PCR from retina, undifferentiated (Und) and muscle-differentiated (Diff) BC3H1 cells. Images represent ethidium bromide-stained agarose gels loaded with PCR reaction products after RT-PCR.

3.3.3. *LTx2 action on Ca^{2+} channels*

BC3H1 cells were loaded with Fluo-3-AM and visualized by confocal microscopy in the presence of the LTx2 without or with Na^+ channel blocker tetrodotoxin (1 μM, TTX) (Fig. 6). Normal Ca^{2+} oscillations (Fig. 6, upper panel) are mediated by L-type Ca^{2+} channels and activating sarcoplasmic/endoplasmic reticulum Ca^{2+}–Mg^{2+}–ATPase (SERCA) inducing action potentials [7,19,24,37], and can be used as antagonists screening with toxins. When Na^+ channel-induced membrane depolarization was blocked, Ca^{2+} channels were the only alternative for inducing membrane depolarization. We noted that spontaneous $[Ca^{2+}]_i$ oscillations were abolished and that there was a decrease in the basal level of $[Ca^{2+}]_i$ in the presence of 80 μM LTx2 and 1 μM TTX (Fig. 6, lower panel). BC3H1 cells had Ca^{2+} oscillations before LTx2 was added to bathing medium, even in the presence of TTX (Fig. 6, lower panel). These data are consistent with another study [21] that showed similar results with extracted venom, suggesting the presence of toxins that block L-type Ca^{2+} channels.

3.4. *Expression of RyR, InsP$_3$R and VGCCs in BC3H1 cells*

Above results indicate that several kinds of ion channels function as Ca^{2+} signaling pathways in BC3H1 cells. Therefore, we examined the mRNA expression for ion channel genes (RyR I, II, and III; InsP$_3$R I, II, and III, VGCC α-subunits) using RT-PCR. RyR type I gene was only detectable in muscle-differentiated stage (Fig. 7A). InsP$_3$R I, II, and III genes were expressed at detectable levels in undifferentiated and muscle-differentiated BC3H1 cells (Fig. 7B). For the VGCCs, the expression of dihydropyridine receptors (DHP receptors), L-, T-, and P/Q, N, R-types were examined. The results related to DHP receptor showed that undifferentiated stage of BC3H1 cells express only CaV1.3α1 isoform. Otherwise, in muscle-differentiated BC3H1 cells

only the N-type Ca^{2+} channel could not be detected (Fig. 7D–F).

4. Discussion

4.1. Ca^{2+} oscillation and Ca^{2+} release from ER in BC3H1 cells

Spontaneous $[Ca^{2+}]_i$ oscillations evoked by Ca^{2+}-mobilizing stimuli are present in many types of non-excitable cells, such as pancreatic acinar cells [23,27], oocytes [20], liver cells, and fibroblasts [8]. As shown in Fig. 3, BC3H1 cells showed spontaneous $[Ca^{2+}]_i$ oscillations without agonists stimuli (Fig. 3A). Our data obtained in Ca^{2+}-free external buffer (Fig. 3A) and with Ca^{2+} pump ATPase inhibitors (Fig. 3B and C) clearly indicate that the intracellular Ca^{2+} store is the main source of Ca^{2+} for $[Ca^{2+}]_i$ oscillations. However, Ca^{2+} influx is required to maintain these Ca^{2+}oscillations, which can refill the intracellular Ca^{2+} stores by influx across the plasma membrane. Then, the decrease of amplitudes of $[Ca^{2+}]_i$ oscillations in Ca^{2+}-free external buffer (Fig. 3B) may be explained by absence of Ca^{2+} influx.

$InsP_3R$ and RyR receptors are known to participate in release of Ca^{2+} from the intracellular stores [8], and have been suggested to explain the mechanisms of $[Ca^{2+}]_i$ oscillations [13]. It has been proposed that $[Ca^{2+}]_i$ oscillations are generated by either fluctuating or sustained concentrations of cytosolic $InsP_3$ [5]. Recently, it was reported that $[Ca^{2+}]_i$ fluctuations are induced by $InsP_3$ levels through a dynamic and rapid uncoupling of G-protein coupled receptors [26]. This finding could explain our results of $[Ca^{2+}]_i$ oscillations and calcium entry through by plasma membrane, but additional studies are necessary.

This is the first work which presents the nature and functional roles of the intracellular Ca^{2+} stores in BC3H1 cells. It is not known whether a caffeine/ryanodine-sensitive store exists in BC3H1 cells. We demonstrated Ca^{2+} release from ER via $InsP_3Rs$ (Fig. 3B and C). However, because caffeine presented no effect in $[Ca^{2+}]_i$, in BC3H1 cells (Fig. 4C) and because the expression of RyRs mRNA is absent (Fig. 7A), we suggest that RyRs have a minor contribution if any contribution to Ca^{2+} release from internal stores. Taken together, our results demonstrate that $InsP_3Rs$ are the major source to Ca^{2+} release from ER in BC3H1 cells and that RyRs mRNA seem not to be expressed in this cell line at this stage. It has been described that at early stages of development $InsP_3R$ mRNA and functional $InsP_3$-gated Ca^{2+} release channels are widely expressed in virtually all tissues in mouse embryos, but RyR mRNA could only be detected in the myotome [34]. Therefore, we could speculate that functional RyRs might be present during or after differentiation to excitable cells.

4.2. Ca^{2+} entry pathway in BC3H1 cells and LTx2 effect

Calcium influx through the plasma membrane plays a central role in controlling cellular activities. In spite of intensive research, there is no consensus yet on how Ca^{2+} entry is controlled in non-excitable cells. In most non-excitable cells examined, the existence of SOC entry has been demonstrated [10]. In this study, we first demonstrated the functional expression of SOCs in BC3H1 cell line and the role of LTx2 toxin (Fig. 5D and Fig. 6). We also evaluated whether functional VGCCs are present in this cell line. We conclude here, that Ca^{2+} entry through plasma membrane is mainly mediated by the SOCs receptors in BC3H1 cell line and that LTx2 blocks L-type Ca^{2+} channels.

Given that LTx1, LTx2 and LTx3 have very similar structures, differing from one another by only 1–3 residues [40] it is likely that LTx1 and LTx3 also act on Ca^{2+} channels. However, only the expression and biological characterization of the recombinant of LTx1 and LTx3 toxins can reveal their molecular targets.

Acknowledgments

This work was supported by grants from Fundação de Amparo à Pesquisa do Estado de Minas Gerais (FAPEMIG)—Contract no. CBB 718/05 and Contract no. CBB APQ-4615-4.01/07, PRONEX and by Conselho Nacional de Desenvolvimento Científico e Tecnológico Process 471080/2006-3. R.R. Resende is supported by a postdoctoral research fellowship from FAPESP. English editing has been performed throughout the text by native English speaker Avishek Adhikari from Department of Biological Sciences, Columbia University, New York, USA.

REFERENCES

[1] Agrawal N, Malhotra P, Bhatnagar RK. Interaction of gene-cloned and insect cell-expressed aminopeptidase N of *Sdoptera litura* with insecticidal crystal protein Cry1C. Appl Environ Microb 2002;68:4582–92.
[2] Altschul SF, Madden TL, Shaffer AA, Zhang J, Zhang Z, Miller W, et al. Gapped BLAST and PSI-BLAST: a new generation of protein database search programs. Nucleic Acids Res 1997;25:3389–402.
[3] Berridge MJ. Inositol trisphosphate and calcium signaling. Nature 1993;361:315–25.
[4] Berridge MJ. Elementary and global aspects of calcium signaling. J Physiol 1997;499:291–306.
[5] Berridge MJ, Lipp P, Bootman MD. The versatility and universality of calcium signaling. Nat Rev Mol Cell Biol 2000;1:11–21.
[6] Bradford MM. A rapid and sensitive method for the quantification of microgram quantities of protein utilizing the principle of protein–dye binding. Anal Biochem 1976;72:248–54.
[7] Bultynck G, De Smet P, Weidema AF, Ver Heyen M, Maes K, Callewaert G, et al. Effects of the immunosuppressant FK506 on intracellular Ca^{2+} release and Ca^{2+} accumulation mechanisms. J Physiol 2000;525:681–93.
[8] Clapham DE. Calcium signaling. Cell 1995;80:259–68.
[9] Corzo G, Gilles N, Satake H, Villegas E, Dai L, Nakajima T, et al. Distinct primary structures of the major peptide toxins from the venom of the spider *Macrothele gigas* that bind to sites 3 and 4 in the sodium channel. FEBS Lett 2003;547:43–50.
[10] Elliot AC. Recent developments in non-excitable cell calcium entry. Cell Calcium 2001;30:73–93.
[11] Escoubas P, Celerier ML, Romi-Lebrun R, Nakajima T. Two novel peptide neurotoxins from the venom

on the tarantula *Lasiodora parahybana*. Toxicon 1997;35: 805–6.
[12] Escoubas P, Diochot S, Corzo G. Structure and pharmacology of spider venom neurotoxins. Biochimie 2000;82:893–907.
[13] Fewtrell C. Ca^{2+} oscillations in non-excitable cells. Annu Rev Physiol 1993;55:427–54.
[14] Guatimosin SCF, Prado VF, Diniz CR, Chávez-Olórtegui C, Kalapothakis E. Molecular cloning and genomic analysis of TsNTxP; an immunogenic protein from *Tityus serrulatus* scorpion venom. Toxicon 1999;37:507–17.
[15] Guette C, Legros C, Tournois G, Goyffon M, Célérier M-L. Peptide profiling by matrix assisted laser desortion/ ionisation time-of-flight mass spectrometry of the *Lasiodora parahybana* tarantula venom gland. Toxicon 2006;47:640–9.
[16] Grynkiewicz G, Poenie M, Tsien RY. A new generation of Ca^{2+} indicators with greatly improved fluorescence properties. J Biol Chem 1985;260:3440–50.
[17] Hallett MB, Dormer RL, Campbell AK. In: Siddle K, Hutton JC, editors. Peptide hormone action: a practical approach. New York: Oxford University Press; 1990. p. 115–50.
[18] Kalapothakis E, Kushmerick C, Gusmão DR, Favaron GOC, Ferreira AJ, Gomez MV, et al. Effects of the venom of a Mygalomorph spider (*Lasiodora* sp.) on the isolated rat heart. Toxicon 2003;41:23–8.
[19] Kidokoro Y. Spontaneous calcium action potentials in a clonal pituitary cell line and their relationship to prolactin secretion. Nature 1975;258:741–2.
[20] Kiselyov K, Xu X, Mozhayeva G, Kuo T, Pessah I, Mignery G, et al. Functional interaction between InsP3 receptors and store-operated Htrp3 channels. Nature 1998;397:255–9.
[21] Kushmerick C, Carvalho FM, de Maria M, Massensini AR, Romano-Silva MA, Gomez MV, et al. Effects of a *Lasiodora* spider venom on Ca^{2+} and Na^{+} channels. Toxicon 2001;39:991–1002.
[22] Laemmli UK. Cleavage of structural proteins during the assembly of the head of bacteriophage T4. Nature 1970;227:680–5.
[23] LeBeau AP, Yule DI, Globlewski GE, Sneyd J. Agonist-dependent phosphorylation of the inositol 1,4,5-trisphosphate receptor: a possible mechanism for agonist-specific calcium oscillations in pancreatic acinar cells. J Gen Physiol 1999;113:851–72.
[24] Mackrill JJ, Challiss RA, O'Connell DA, Lai FA, Nahorski SR. Differential expression and regulation of ryanodine receptor and myo-inositol 1,4,5 trisphosphate receptor Ca^{2+} release channels in mammalian tissues and cell lines. Biochem J 1997;327:251–8.
[25] McPherson PS, Campbell KP. Characterization of the major brain form of the ryanodine receptor/Ca^{2+} release channel. J Biol Chem 1993;268:19785–90.
[26] Nash MS, Young KW, Challiss RS, Nahorski SR. Intracellular signalling. Receptor-specific messenger oscillations. Nature 2001;413:381–2.
[27] Osipchuk YV, Wakui M, Yule DI, Gallacher DV, Petersen OH. Cytoplasmic Ca^{2+} oscillations evoked by receptor stimulation, G-protein activation, internal application of inositol triphosphate or Ca^{2+}: simultaneous microfluorimetry and Ca^{2+} dependent Cl^{-} current recording in single pancreatic acinar cells. EMBO J 1990;9:697–704.
[28] Parekh AB, Penner R. Store depletion and calcium influx. Physiol Rev 1997;77:901–30.
[29] Penaforte CL, Prado VF, Prado MAM, Romano-Silva MA, Guimarães PEM, Gomez MV, et al. Molecular cloning of cDNAs encoding insecticidal neurotoxic peptides from the spider *Phoneutria nigriventer*. Toxicon 2000;38:1443–9.
[30] Rash LD, Hodgson WC. Pharmacology and biochemistry of spider venoms. Toxicon 2002;40:225–54.
[31] Resende RR, Gomes KN, Adhikari A, Britto LRG, Ulrich H. Mechanism of acetylcholine-induced calcium signaling during neuronal differentiation of p19 embryonal cells in vitro. Cell Calcium 2008;43:107–21.
[32] Resende RR, Majumder P, Gomes KN, Brittto LRG, Ulrich H. P19 embryonal carcinoma cells as in vitro model for studying purinergic receptor expression and modulation of N-methyl-D-aspartate-glutamate and acetylcholine receptors during neuronal differentiation. Neuroscience 2007;146:1169–81.
[33] Roberto PG, Kashima S, Soares AM, Chiobato L, Faça VM, Fuly AL, et al. Cloning and expression of an acidic platelet aggregation inhibitor phospholipase A_2 cDNA from *Bohtrops jararacussu* venom gland. Protein Expr Purif 2004;37: 102–8.
[34] Rosemblit N, Moschella MC, Ondriasá E, Gutstein DE, Ondrias K, Marks AR. Intracellular calcium release channel expression during embryogenesis. Dev Biol 1999;206: 163–77.
[35] Sambrook J, Fritsh EF, Maniatis T. Molecular cloning: a laboratory manual, 2nd ed., New York: Cold Spring Harbor Laboratory Press; 1989.
[36] Sanger F, Nicklen S, Coulson AR. DNA sequencing with chain termination inhibitors. Proc Natl Acad Sci USA 1977;74:5463–7.
[37] Schlegel W, Winiger BP, Mollard P, Vacher P, Wuarin F, Zahnd GR, et al. Oscillations of cytosolic Ca^{2+} in pituitary cells due to action potentials. Nature 1987;329:719–21.
[38] Schubert D, Harris AJ, Devine CE, Heinemann S. Characterization of a unique muscle cell line. J Cell Biol 1974;61:398–413.
[39] Sine SM, Taylor P. Functional consequences of agonist-mediated state transitions in the cholinergic receptor. Studies in cultured muscle cells. J Biol Chem 1979;254: 3315–25.
[40] Vieira ALG, Moura MB, Babá EH, Chávez-Olórtegui C, Kalapothakis E, Castro IM. Molecular cloning of toxins expressed by the venom gland of *Lasiodora* sp.. Toxicon 2004;44:949–52.
[41] Wu J, Kamimura M, Takeo T, Suga S, Wakui M, Maruyama T, et al. 2-Aminoethoxydiphenyl borate modulates kinetics of intracellular Ca^{2+} signals mediated by inositol 1,4,5-trisphosphate-sensitive Ca^{2+} stores in single pancreatic acinar cells of mouse. Mol Pharmacol 2000;58:1368–74.